

INVESTIGATION ON THE INFLUENCE OF POST WELD HEAT TREATMENTS ON WELDMENTS BETWEEN P91 AND P11

E. S. Mosa¹, Hussein. M. Abdelaziz¹, M. A. Morsy², A. E. Abd elmaoula¹, A. Atlam¹

(1) Al Azhar University, Faculty of Engineering , Mining and Petroleum Engineering Department, Egypt.

(2) Central Metallurgical Research and Development Institute (CMRDI), Egypt.

ABSTRACT - This work aims at optimizing post weld heat treatment (PWHT) conditions of weld joint between P11 (1.1 Cr) and P91 (9 Cr) steels; using E9015B9/ER90SB9 as filler metals. The PWHT was conducted at 750°C and 850 °C for holding times 0.5, 1 and 2 hours. The results indicated that: PWHT at 750°C for 0.5 hour was the proper conditions to obtain optimum grain size and regular Hardness distribution of heat affected zone (HAZ).

Key Words: P11, P91, Post weld heat treatment, Microstructure, Hardness, Heat Affected Zone, fresh martensite.

1. INTRODUCTION

Post weld heat treatment (PWHT) is considered the most common technique employed for relieving; the residual stresses generated from welding processes and final fabrication process of many engineering components. In spite of mechanical properties of weldments are usually enhanced by heat treatment, a degradation of some material properties can also be occurred especially creep properties and tensile strength in the case of multi PWHT cycles [1,2]. The HAZ is the region in the Weldment that does not melt but is altered in microstructure and material properties due to the cyclic heating and cooling of the welding process. It lies between the fusion line of the weld deposit and the base metal. Within the HAZ there are regions of distinct microstructure that form due to the peak temperatures reached in the welding process. The HAZ contains a coarse-grained region (CGHAZ) near the fusion line, a fine-grained (FGHAZ) region in the center and a fine-grained inter-critical region (ICHAZ) near the base metal. These regions are created when the localized heat from welding exceeds the Ac1 critical temperature, transforming the steel microstructure from martensite to austenite [3, 4]. The degree of microstructural change depends on the maximum heat exposure and the cooling rate, both of which are dependent on the distance from the fusion line. These variable factors allow for a wide range of microstructure across the HAZ.

P11 (14 Cr - 12 Mo) was a ferritic steel used for installation in critical power plant piping systems since the early 1940's however P91 (9Cr-1Mo-V) was developed by in the late 1970's, to further improve the creep strength. P91's microstructure is martensitic as compared to the bainitic

structure of P11 alloy steels. This difference in chemical composition and microstructure between P11 and P91 makes post weld heat treatment of joint between them can pose a challenge, where appropriate heat treatment for one component of the weldment may be deleterious for the other. The aim of this research work is to determine the suitable PWHT conditions, which provides the proper microstructure and hardness to avoid earlier component failure; for long-term high temperature service. [5]

J.G. Nawrocki, et al. Investigated the effect of Post weld Heat-Treatment Response of Simulated Coarse-Grained Heat-Affected Zones in 2.25Cr-1Mo (HCM2S) Ferritic Steel and found The CGHAZ of HCM2S and 2.25Cr-1Mo steels experienced secondary hardening after tempering at 575 8C for 5 hours. A large amount of intragranular Fe-rich M3C carbides provided the hardening in 2.25Cr-1Mo steel and a dense distribution of small (5 to 20 nm), intragranular W-rich carbides provided the hardening in HCM2S. The hardness of HCM2S was more stable than that of 2.25Cr-1Mo steel at longer tempering times and higher temperatures, due to the precipitation of W- and V-rich carbides, which strengthened the prior-austenite grain interiors and stabilized the lath structure. [6]

J. Ohlsson studied the Effects of different heat treatments on hardness of Grade 91 steel and found the following When heat treating the Grade 91 material there is no significant benefit attained from putting it through several cycles, one heat treatment cycle is enough and PWHT's a soaking temperature of 750° C is what generates the most stable hardness profile when measuring the hardness over the base material, HAZ and the weld. A PWHT at 750° C does not make the weld to hard nor the base material to soft and when heat treating components that vary in thickness the soaking temperature does not seem essential to the obtained hardness. [7]

2- EXPERIMENTAL PART:

Base metals: pipe with 6 in. dia., 10mm thick. of alloy P11 and P91, chemical composition and mechanical properties of the present test coupon are given in Table 1 and Table 2 respectively.

Filler metals: AWS ER90SB9 filler wires for the first two root passes and AWS E9015B9 electrodes for the subsequent filler passes. Chemical compositions of filler metals are shown in Table 3

Joint geometry: the dimensions of the test coupon where butt joint with single V-groove was used.

Welding parameters: the parameters are given in Table 4 where preheating was maintained between 268°C – 288°C, and inter pass temperature was controlled to be at 300°C. An intermediate post weld heat treatment for 0.30 hr. at 350°C was conducted immediately after welding.

PWHT: Different ranges of holding temperatures and holding times were used as shown in Table 5 where sex heat treatment cycles were tabulated to cover a wide range of applications.

Microstructure characterization:

Microstructure Characterization was performed using optical metallography and scanning electron microscope (SEM). The specimens were ground and polished using standard metallographic technique, and afterwards etched in a Vilella’s Reagent (25 ml ethanol, 1.5ml HCl and 0.3 g Picric acid) Picric acid is mixed with ethanol then HCl is added. Microhardness was measured for across weld metal HAZ

Mechanical properties:

Tension test: For each welding procedure; two specimens for transverse tensile test were cut and prepared in accordance with ASME-Section IX, item QW-150. The acceptance criteria are the minimum specified tensile strength of the base metal.

Guided-bend test: For each welding procedure; four specimens for transverse side bend test were be prepared by cutting the test pipe in accordance with ASME-Section IX, item QW-160. The specimens have approximately rectangular cross section with 10mm thickness. The acceptance criteria is that: the guided-bend specimens shall have no open discontinuity in the weld or heat-affected zone exceeding 3 mm, measured in any direction on the convex surface of the specimen after bending.

Table 1: Chemical analysis (Wt%) of P11and P91steels.

Steel Grade	C	Si	Mn	P	S	Ni	Cr
P11	0.13	0.53	0.52	0.01	0.001	0.06	1.1
	Mo	Al	V	Nb	N	Cu	
	0.46	0	0	0	0	0	
P91	C	Si	Mn	P	S	Ni	Cr
	0.1	0.25	0.33	0.0125	0.002	0.13	8.5
	Mo	Al	V	Nb	N	Cu	
	0.89	0.002	0.22	0.079	0.042	0.03	

Table 2: Mechanical properties of the P91 steel.

Property	P11	P91	
Tensile Test	U.T.S, MPa	415	675
	El. %	14	23.5
Av. Hardness (HV)	152	210	

Table 3: Chemical analysis (wt%) of AWS ER90S-B9 and AWS E9015-B9.

Filler Metal	C	Si	Mn	P	S	Ni	Cr
AWS ER90S-B9	0.09	0.15	0.45	0.006	0.0015	0.7	8.9
	Mo	Cu	Al	V	Nb	N	
	0.8	0.01	0.01	0.2	0.1	0.03	
AWS E9015-B9	C	Si	Mn	P	S	Ni	Cr
	0.11	0.13	0.85	0.01	0.0053	0.95	8.4
	Mo	Cu	Al	V	Nb	N	
	1.12	0.0011	0.23	0.22	0.09	0.053	

Table 4. Summary of welding procedures used during pipes welding by E9015B9/ER90SB9.

Process/ Layer No.	Electric current		Average Voltage	Preheating Temp., °C	Filler Metal / Electrode	
	Type/ Polarity	AMP. Average			Type	Dia. (mm)
Sample 1						
GTAW (Root)	DC / EN	112.8	12.7	219	ER90S-B9	2.4
SMAW (1)	DC / EP	137	22.73	230	E9015-B9	2.5
SMAW(2 - 7)	DC / EP	137	22.73	230	E9015-B9	2.5
Total No. of Passes = 8						

Table 5: heat treatment cycles

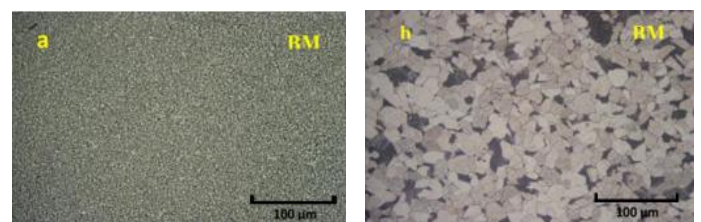
Cycle No.	Heating Rate (°C /Hr)	Soaking Time. (Minutes)	Soaking Temp. (°C)	Heating Rate (°C /Hr)
A	80	30	750	80
B		60		
C		120		
D	30	850		
E	60			
F	120			

3. RESULTS AND DISCUSSION

3.1. Microstructure Evolution

3.1.1 Microstructure Evolution before Welding

Microstructure of base metals; P91 and P11 is revealed in Fig.1a, and Fig.1b respectively. It can be noted that



microstructure of P11 is ferrite/pearlite however microstructure of P91 is tempered martensite[8] .

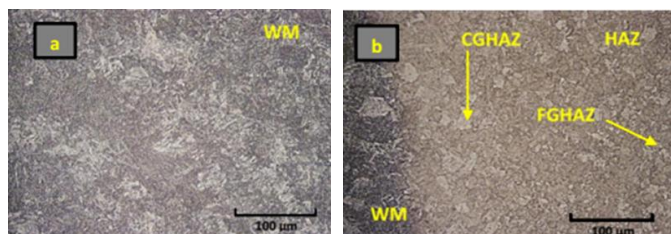
(a). Base Metal of P91 (b). Base Metal of P11
Figure (1a, b) P91 and P11 base metal microstructures

3.1.2 Microstructure in as weld condition.

Microstructure of P91weld metal is shown in Fig. 2a where coarse acicular martensite is observed however HAZ microstructure of P91 is represented in Fig. 2b and Fig. 3 and Fig. 3a revealing un-tempered martensitic phase with different grain size. [9, 10]. HAZ microstructure of P11 is also

illustrated in Fig. 4, showing that grain coarsening zone and refinement zone with bainitic structure as predominate structure. the bainitic structure is observed in coarse grains however grain refinement zones have a spheroidized pearlite. In spite of grain boundaries of as weld un-tempered martensite and bainite are hardly noted; many researches [8] were published demonstrating that within the HAZ there are regions of distinct microstructure that form due to the peak temperatures reached in the welding process. The HAZ contains a coarse-grained region (CGHAZ) near the fusion line, a fine-grained (FGHAZ) region in the center and a fine-grained inter-critical region (ICHAZ) near the base metal. These regions are created when the localized heat from welding exceeds the Ac1 critical temperature, transforming the steel microstructure from martensite to austenite [9,10]. The degree of microstructural change depends on the maximum heat exposure and the cooling rate, both of which are dependent on the distance from the fusion line. These variable factors allow for a wide range of microstructure across the HAZ. The grain coarsening is occurred due to carbide decomposition resulting in no carbide inhibiting grain growth [8].

The above results are supported by hardness distribution measured across the weld and both HAZs. Hardness measurements are shown in Fig.20 where hardness of weld metal is ranged from 350 to 400 HV reflecting the martensitic structure of weld metal. The hardness is decreased slightly across HAZ of P91 until tempered martensite of base metal. In other side where HAZ of P11 the hardness is sharply reduced where bainitic structure is founded.



(a). Weld metal of P91
(b). HAZ of P91 in as weld condition

Figure 2. Weld metal and HAZ microstructures of P91 after welding by ER90S-B9/ E9015-B9.

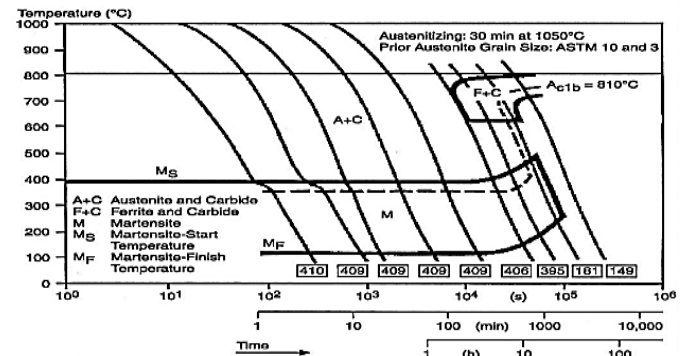
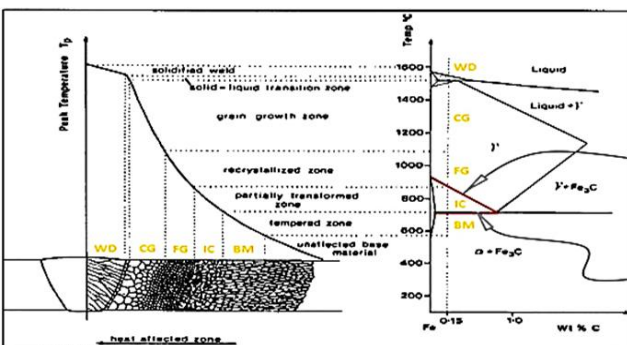
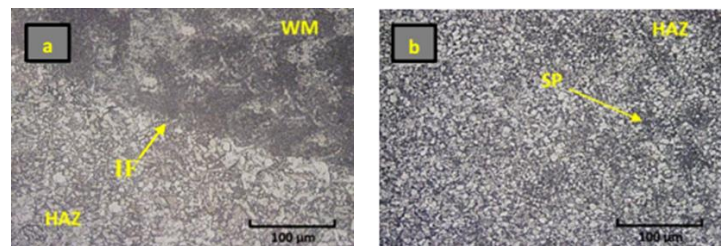


Figure 3: Schematic representations of microstructures



developed in weld metal and HAZ as function of peak temperature during welding of P91 [9, 10].

Figure 3a: CCT diagram of P91 steel [11].

(a). HAZ and Interface of P11 (b). HAZ of P11
Figure 4. P11 Microstructures after welding by ER90S-B9/ E9015-B9 filler metal

3.1.3. Microstructure of steel weldment after PWHT 3.1.3.1 Microstructure of steel weldment after PWHT at 750°C

Figures 5 illustrate the microstructure of P91 base metal after post weld heat treatment at 750°C for holding times 0.5, 1.0 and 2.0 hours, respectively. It is noticed from this figure that all received microstructures were tempered Martensite. And there is no significant change in microstructural that observed using this temperature for different time. The same results were obtained by Tammasophon et al. [8] and Ma. Allam [12]. Typical characteristics were also found in HAZ after PWHT; as shown in Figures 5. However, the grain structures of temper Martensite of post weld heat treated HAZ are finer than those of post weld heat treated base metal microstructures. The microstructures of post weld heat treated interface zone adjacent to weld metal after heating at a temperature of 750°C are shown in figures 6a, b, and c, at holding times 0.5, 1.0 and 2.0 hours, respectively. Heat treatment resulted in tempering of the martensitic structure in both of weld metal, heat affected zone and base metals. This result is supported by the hardness distribution results that discussed in section 3.2.1. 2.1.

Figure 7 show the microstructure of P11 base metals after applying post weld heat treatment at temperature of 750°C for holding times 0.5, 1 and 2 hours, respectively. All these

microstructures consist of ferrite and ferrite with carbides (pearlite). No significant effect of different PWHT durations on the microstructure was found.

Figures 8a, b and c, d show HAZ microstructure after PWHT at 750°C for holding times 0.5, 1.0 and 2.0 hours, respectively. No significant affects in grain refining size with PWHT duration. Furthermore interface (IF) microstructures of P11 connecting to weld metal after PWHT was done at 750°C for holding times 0.5, 1.0 and 2.0 hours, respectively are illustrated in same figures.

In general, the microstructures consist of more coarsening grain structures occurring at high sufficient level of welding heat to transform the structure to coarsen austenite grains structure, and cooled down later to be coarsening bainite grain structure instead. However, after PWHT at 750 °C, all microstructures would transform again to ferrite structure with carbide precipitation. From Figure.8 and tables 6, 7 and 8 it is clear that, the grain size increases with increasing the soaking time. The same result was obtained in welding of P22 [8]. This result is supported by the hardness distribution results that illustrated in section 3.2.1.2.1.

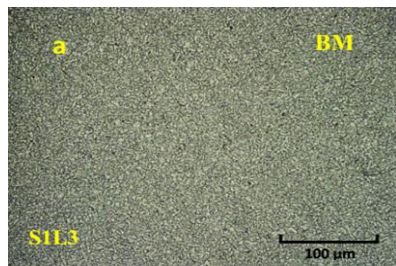
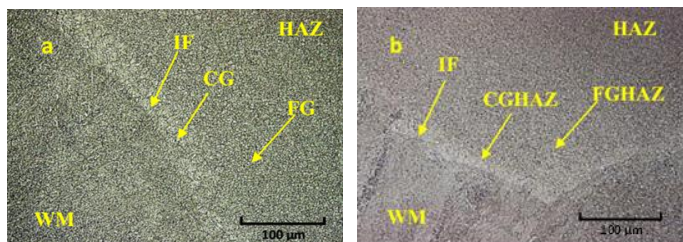
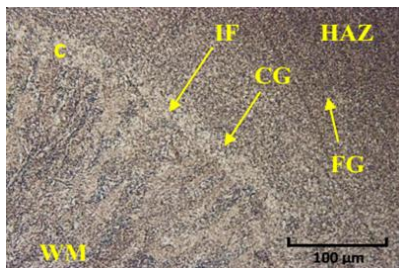


Figure 5. Microstructures of P91 steel base metal after PWHT at 750°C.



(a). (S1L3) 0.5 hour

(b). (S1L5) 1.0 hour



(c). (S1L7) 2.0 hours

Figure 6. Microstructures of P91 steel base metal after PWHT at 750°C and using ER90S-B9/ E9015-B9 as filler metal at different holding times

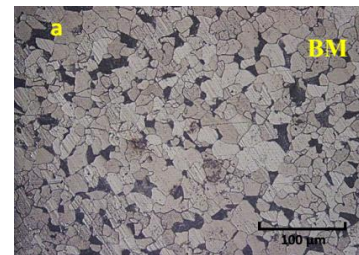
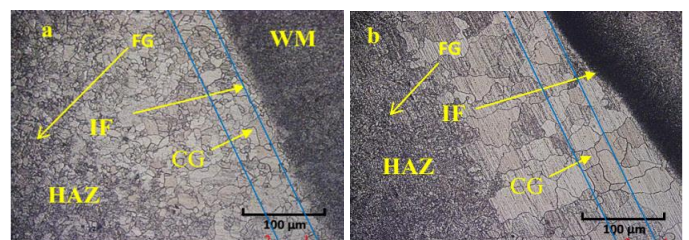
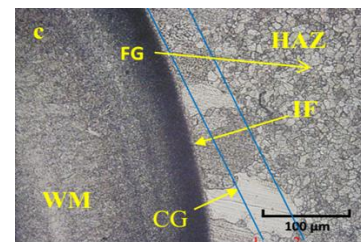


Figure 7. Microstructures of P11 steel base metal after PWHT at 750°C.



(a). (S1L3) I.F 0.5 hour

(b). (S1L5) IF 1.0 hour



(c). (S1L7) IF 2.0 hours

Figure 8. Microstructures of HAZ and IF (inter face zone) P11 by using ER90S-B9/ E9015-B9 as filler metal after PWHT at 750 OC at different holding times.

Table 6- Calculation of ASTM number for P11 appeared in Fig.12a using Intercept method (ASTM E112) [13]

Field of view	Test line length (L, mm)	Number of Intercept (P)	*P _i (mm) ⁻¹
1	50	30	96
2	50	33	105.6
Average			100.8
Average ASTM number = -3.3+6.65 log (P _i)			10

Table 7- Calculation of ASTM number for P11 appeared in Fig.12b using Intercept method (ASTM E112) [13]

Field of view	Test line length (L, mm)	Number of Intercept (P)	*P _i (mm) ⁻¹
1	50	14	44.8
2	50	16	51.2
Average			48
Average ASTM number = -3.3+6.65 log (P _i)			7.9

Table 8- Calculation of ASTM number for P11 appeared in Fig.12c using Intercept method (ASTM E112)[13]

Field of view	Test line length (L, mm)	Number of intercept (P)	*P _L (mm) ⁻¹
1	50	9	28.8
2	50	15	48
Average			38.4
Average ASTM number = $-3.3+6.65 \log (P_i)$			7.2

*P_L is Number of intercepts per unit length multiplied by magnification

3.1.3.2 Microstructure of steel weldment after PWHT at 850°C

Figure 9 show microstructures of P91 base metal after applying post weld heat treatment at 850°C at different holding times of 0.5, 1.0 and 2.0 hours, respectively. It is clear that the microstructures consist of over tempered Martensite. And the microstructure of HAZ shows coarse grain zone has seen tempered Martensite. Figs.10a, b and c. show the microstructure at 850°C heat treated, the microstructure significantly tempers; the hardness decreases even more to 175 Hv. As well be discussed in section 3.2.1.2.2. The fine grained HAZ microstructures concern of a fine grained from tempered Martensite as shown in Fig. 10. Inter face zone consist of more coarsening grain from tempered Martensite as shown. in Figs 8a, b and c. This result is supported by the hardness distribution results that discussed later in section 3.2.1.2.2. Weld zone microstructure changes during PWHT to untempered Martensite as shown in Figs.11a, b and c. This could be attributed to the rise of temperature to more than Ac1 transformation temperature. The high Mn and Ni content of weld metal than that of base metal (see Tables 1 and 3) will result in lowering the Ac1 transformation temperature of the weld metal and as a result the austenite is formed and under cooling a untempered Martensite is formed as show in Fig. 8. This was supported by the XRD analysis of the weld metal as shown in Fig. 12. Untempered martensite is formed which rise the hardness of the weld metal to the high value (see section 3.2.1.2.2). The precipitation of Carbide and nitride in the weld metal was suggested by G. Taniguchi et al [14]. This was also supported by the XRD analysis as shown in fig. 12. Where untempered martensite were exist.

Tint etching for weld metal of the specimen shows the existing of newly Martensite as shown in Fig. 13. Scanning electron microscope (SEM) observation of the weld metal after heat treatment at 850°C for holding times 2.0 hours is shown in Fig. 14. Temper martensitic structure with some untempered martensite were also observed. This proved by the rise of weld metal hardness values as will be seen in section 3.2.1.2.2. Point analysis of element distribution in base metal and weld metal are shown in Fig. 15 and Fig. 16 respectively. There is large deference between the analysis of weld metal and base metal. However, a higher Mn and Ni of the weld metal was observed by optical emission spectrometry results as shown in Tables 1 and 3. It is not worthy noting that a higher Mn and Ni content resulted in significant decrease in Ac1 transformation temperature

which my resulted in a formation of untempered martensite that contribute to the rise in hardness of weld metal.

Figure 17 show microstructures of P11 base metals after applying PWHT at a temperature of 850°C for holding times 0.5, 1.0 and 2.0 hours, respectively. All these microstructures consist of ferrite and ferrite with carbides (pearlite) no significant effect of difference in PWHT durations on the microstructure was found. Figures 18a, b and c show the microstructure of HAZ after PWHT at 850°C for holding times 0.5, 1.0 and 2.0 hours, respectively. After post weld heat treated the microstructures of HAZ are much finer than those of post weld heat treated in base metals. Ferrite grains were found in these post weld heat treated HAZ

Figures19a, b and c show the microstructures of P11 interface connecting to weld metal after PWHT was done at 850°C at different holding times 0.5, 1.0 and 2.0 hours, respectively. These obtained microstructures are different from those of P11 HAZ and base metal zones.. However, after applying PWHT at 850°C, all microstructures would transform again to coarsening ferrite structure with carbide precipitation. This results is supported by the results of hardness distribution discussed later in section 3.2.1.2.2. From Fig 19 and tables 9, 10, and 11 grain size increase with increasing the holding times and temperature.

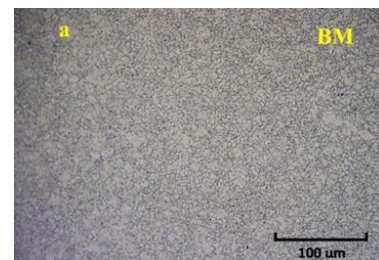
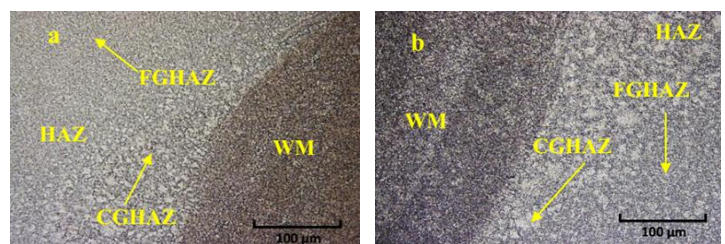


Figure9. Microstructures of P91 steel base metal using ER90S-B9/ E9015-B9 filler metal after PWHT at 850°C.



(a).(S1L9) HAZ G.R/CG 0.5 hr. (b). (S1L11) HAZ GR/C.G1.0 hr.

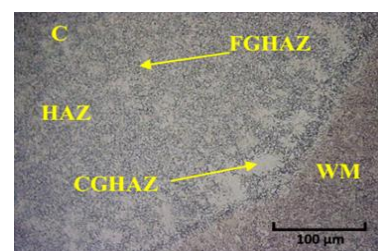
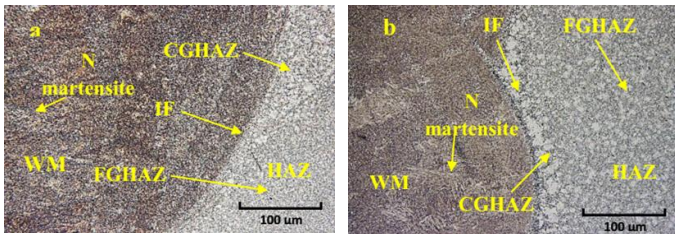
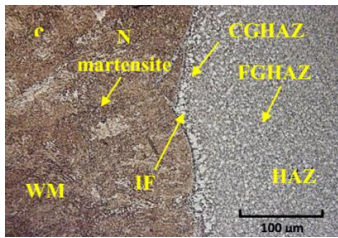


Figure10. Microstructures of P91 steel HAZ using ER90S-B9/ E9015-B9 filler metal after PWHT at 850°C



(a). (S1L9) FW 0.5 hour (b). (S1L11) FW 1.0 hour



(c). (S1L13) FW 2.0 hours

Figure11. Microstructures of weld metal and P91 steel in the region of interface P91 contact weld metal and weld metal after PWHT at 850 °C

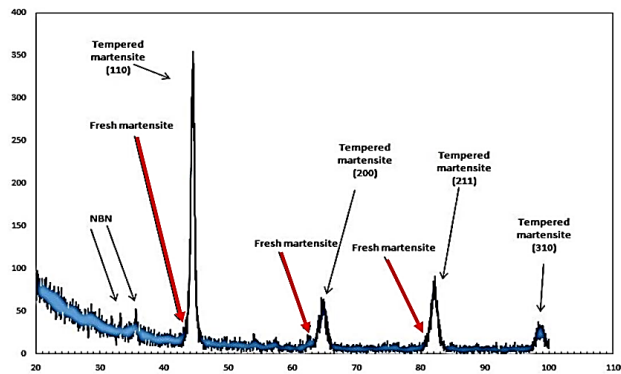


Figure12. XRD spectrum of a specimen treated at 850 °C and 2.0 hrs, showing broadening of peaks, indicated by the arrows, due to un-tempered martensite.

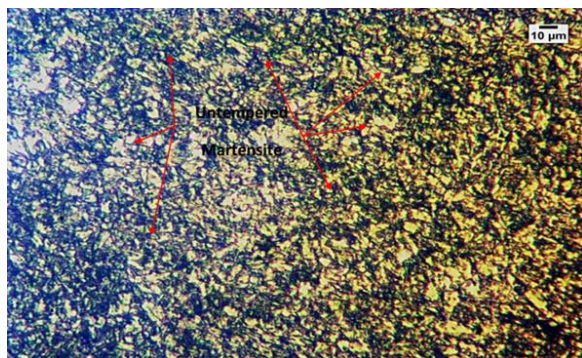


Figure13. Tent etching micro structure of weld metal at 850 °C and 2hrs, showing fresh Martensite.

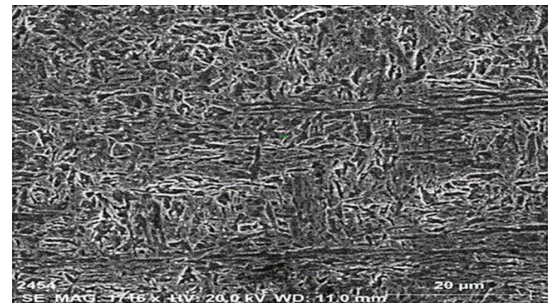


Figure14. SEM for weld metal at 850 °C and 2.0 hrs, showing fresh Martensite.

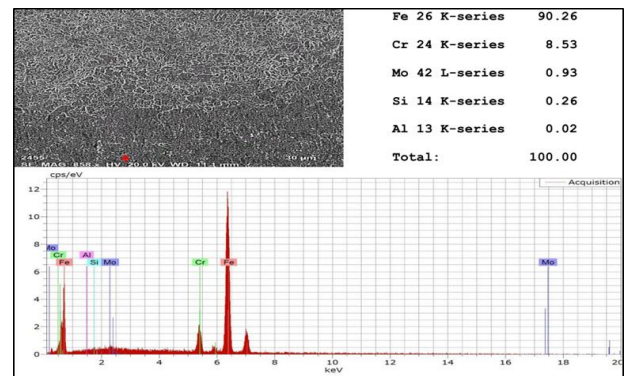


Figure 15. Scanning microscope point analysis for base metal at 850 °C and 2.0 hrs.

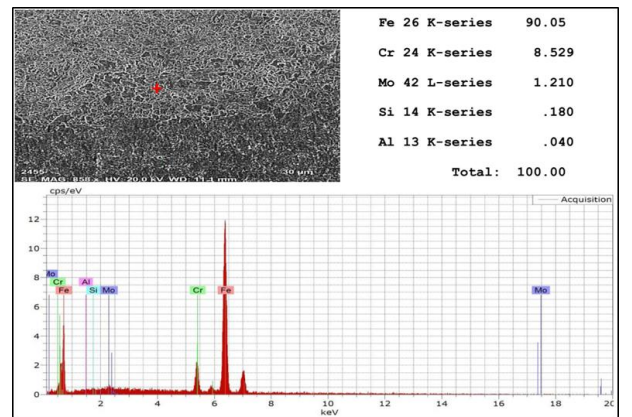


Figure16. Scanning microscope point analysis for weld metal at 850 °C and 2.0 hrs.

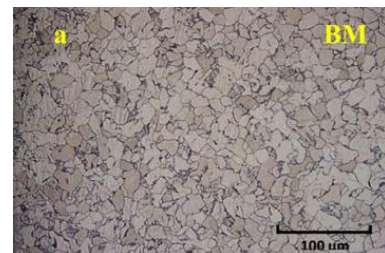
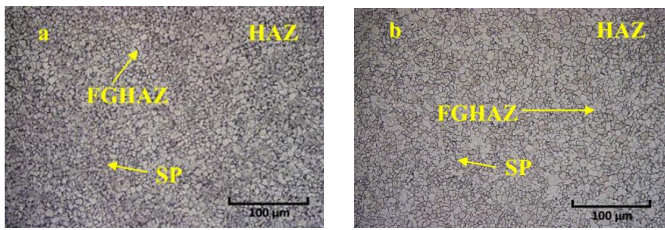
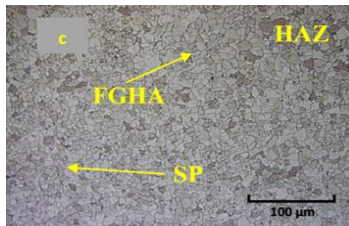


Figure 17. Microstructures of P11 steel base metal after PWHT at 850°C.

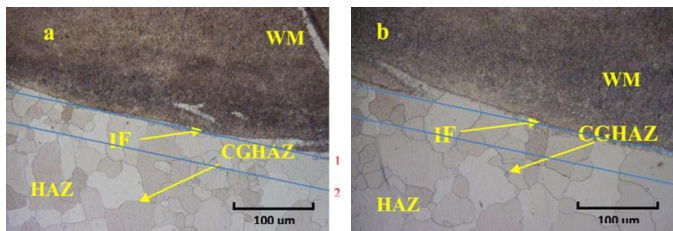


(a). (S1L9) SPHAZ and FG 0.5 hr. (b). (S1L11) SPHAZ and FG 1.0 hr.



(c). (S1L13) SPHAZ and FG 2 hours

Figure18. Microstructures of P11 steel HAZ after PWHT at 850°C.



(a). (S1L9) IF 0.5 hour (b). (S1L11) IF 1.0 hour

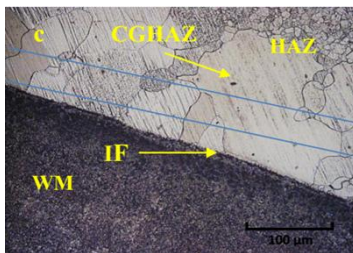


Figure19. Microstructures of IF (inter face) after PWHT at 850 °C

Table 9- Calculation of ASTM number for P11 appeared in 45a using Intercept method (ASTM E112) [13]

Field of view	Test line length (L, mm)	Number of intercept (P)	*P _L (mm) ⁻¹
1	65	17	41.8
2	65	19	46.8
Average			44.3
Average ASTM number = -3.3+6.65 log (P _L)			7.65

Table 10- Calculation of ASTM number for P11 appeared in 45b using Intercept method (ASTM E112) [13]

Field of view	Test line length (L, mm)	Number of intercept (P)	*P _L (mm) ⁻¹
1	65	13	32
2	65	15	36.9
Average			34.5
Average ASTM number = -3.3+6.65log (P _L)			6.93

Table 11- Calculation of ASTM number for P11 appeared in 45c using Intercept method (ASTM E112) [13]

Field of view	Test line length (L, mm)	Number of intercept (P)	*P _L (mm) ⁻¹
1	65	7	17.2
2	65	11	27.1
Average			22.1
Average ASTM number = -3.3+6.65log (P _L)			5.64

*P_L is Number of intercepts per unit length multiplied by magnification

3.2. Mechanical properties:

3.2.1. Hardness testing

3.2.1.1. Hardness testing results after welding:

Figure20 shows hardness profile of welded specimen for sample no. S1L1. The hardness values of HAZ of P91 steel more than 460HV, which is a generally limited hardness of carbon steel HAZ. This is due to the Martensite microstructure as shown in Figs.2 and 4. However; the hardness value of the P11 HAZ was not higher than 205 HV. P91 HAZ has a higher hardness value than P11 HAZ because of its higher hardenability. The interaction between the too high hardness microstructure with hydrogen can result in the crack initiation. This mechanism is well known as hydrogen induced cracking (HIC) [8] Therefore, the post weld heat treatment is needed to reduce this high hardness HAZ.

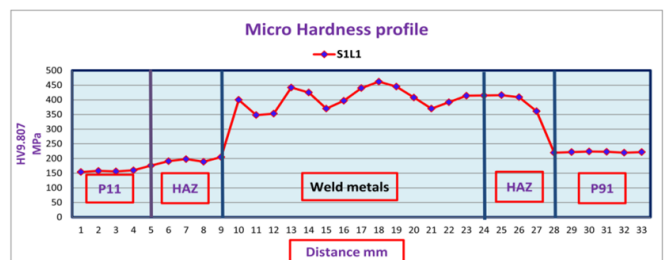


Figure20. Hardness profile of dissimilar weld joint between P91 and P11steel

3.2.1.2. Hardness testing results after PWHT.
3.2.1.2.1. Hardness testing results after PWHT at 750°C :-

Fusion Weld zone microstructure at 750°C and using E9015B9/ER90SB9 as a filler metal changes during PWHT. The as-welded microstructure is a mixture of tempered Martensite and some untempered Martensite, with a 460Hv hardness. PWHT at 750°C for 0.5, 1.0 and 2.0 hr significantly tempers the microstructure, to tempered Martensite. Figures 21a, b and c show the effect of heat treatment temperature on the hardness. The hardness decreases to 300Hv as shown in Figs. 21a and b, and 260Hv in Fig. 21c. The hardness of HAZ of P11 regions consistently decreases as grain coarsening occurs. There is no significant change in base metals hardness.

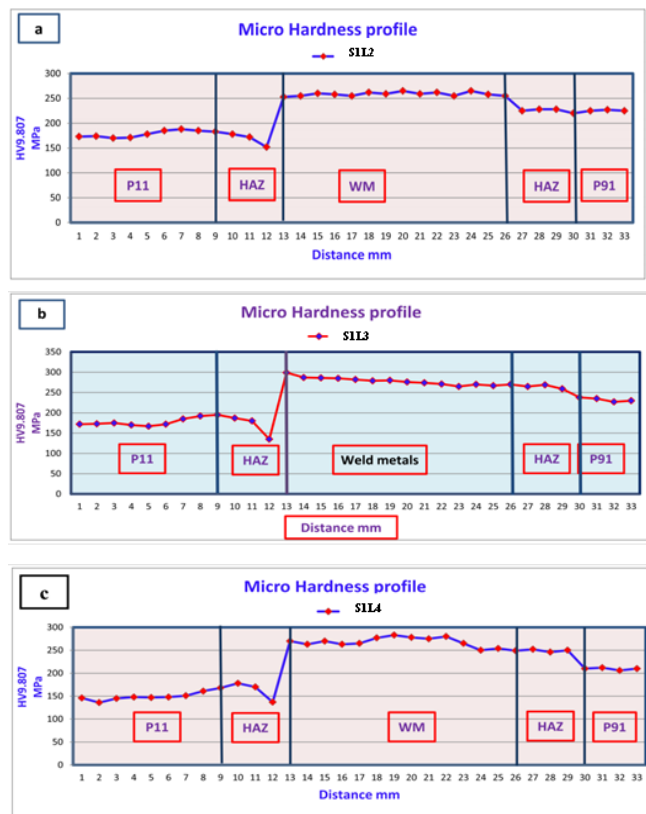


Figure 21. Hardness profile at 750°C for 0.5 hr (a), 1.0 hr (b) and 2.0 hrs (c) soaking time.

3.2.1.2.2. Hardness testing results after PWHT at 850°C:-

Figures 22 a, b and c show the hardness distribution at the base metal, weld metal and HAZ after PWHT at 850°C for 30, 60, 120min. The hardness increased in weld metal to 410Hv. This could be attributed to the formation of untempered martensite as shown in Figs. 11(a, b and c), 12 and 13.

XRD analysis also reveal the formation of fresh martensite with high hardness value as shown in Fig.12 and 22. Also formation of Nitrides could be detected with high hardness value as shown in Fig. 12.

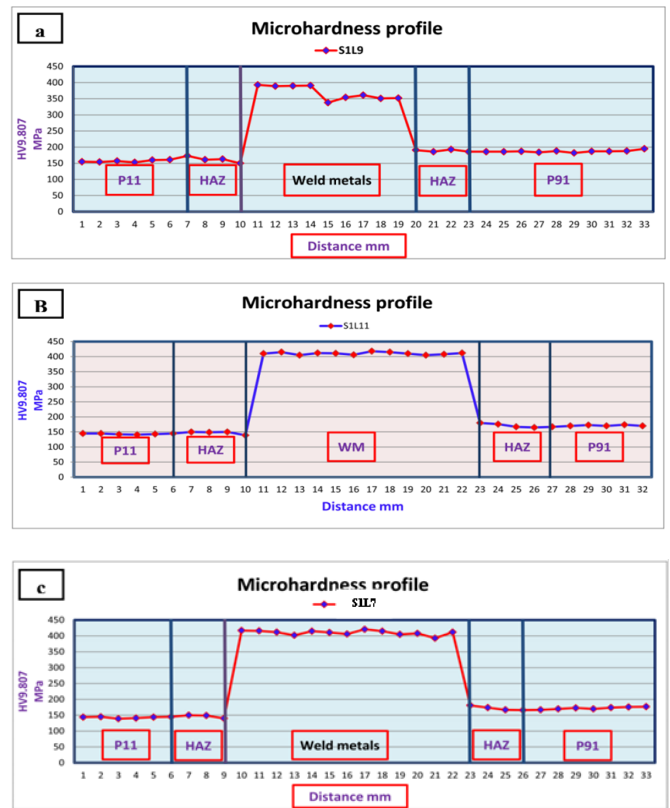


Figure 22. Hardness profile at 850°C 0.5 hr (a), 1.0 hr (b) and 2.0 hrs (c) soaking time.

3.2.2. Tensile testing results:

Figure 23 shows the UTS of the joint studied in the as welded condition and after PWHT using E9015B9/ER90SB9 as a filler metal. The tensile strength decreased with the increase in soaking time. This could be attributed to the grain coarsening and over tempering. All samples were broken in the P11 heat affected zone.

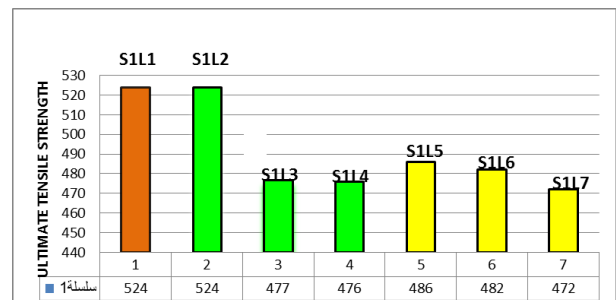


Figure 23. Ultimate tensile strength as welded condition and after heat treated at 750 °C and 850 °C for 0.5hr, 1.0 hr and 2.0 hrs soaking time.

4- CONCLUSIONS

The effect of post weld heat treatment at 750°C for 0.5, 1.0 and 2.0 hours soaking time on microstructures, hardness and tensile strength of TIG and SMAW weldment between the dissimilar weld pipe joints between P11 (1.1Cr) steel and P91 (8.5Cr) steel. Using ER90SB9/E9015B9 as filler metals was studied. The following conclusions can be drawn.

1. After welding, high hardness values in the heat affected zone (HAZ) and weld metal were obtained. This high hardness HAZ was attributed to the transformation of austenite to martensite due to the high cooling rate. The difference in hardness between P91 base metal, heat affected zone and weld metal leading to crack and failure at high temperature during service operation.
2. Post weld heat treatments (PWHT) were found to have a great influence on the obtained microstructure of P91 and P11 weldment which have direct effect on the mechanical properties and weldment serviceability.
3. Tempered martensite was the main observed phase through different areas of P91/P11 weldment. Bainite and ferrite formed.
4. Post weld heat treatment provided more homogeneous microstructures after welding process and reduced the hardness weld metal.
5. the most suitable post weld heat treatment condition for these TIG and SMAW weld joints is at 750°C for 0.5 hours for sample 1. These conditions provide the tensile strength and give the minimum different hardness between weld metal and P91 base metal.
6. Tensile strength decreased with increasing in PWHT temperature and soaking time due to over tempering and grain coarsening.
7. PWHT at 850°C resulted in a significant increase in weld metal hardness at using E9018-B9/ER90S-B9 filler metal. This could be attributed to a formation of newly martensite and/or nitrides that resulted in a significant increase in embrittlement and a significant reduction in impact and toughness.

5- REFERENCES

1. Khaleel Ahmed and J. Krishnan, "Post-weld heat treatment, case Studies, International Symposium on Thermal Spray held at Mumbai May 2-4, 2002, pp. 111 -115.
2. A. Aloraier, R. Ibrahim , P. Thomson, "FCAW process to avoid the use of post weld heat treatment", International Journal Of Pressure Vessels and Piping", 2006,vol.8, pp. 394-398.
3. Benjamin King, "Welding and post weld heat treatment of 2.25%Cr- 1%Mo steel", University of Wollongong, Thesis Collections, <http://ro.uow.edu.au>, theses, 2005, pp. 9-40.
4. Peter Segle, "Numerical simulation of weldment creep response", Doctoral thesis, report KTH / ATM206, Sweden, 2002, pp. 3-4.

5. Christopher Hobbs, Maverick Echivarre, Carly Jania and Stephen Whitson, "Creep Performance and Microstructural Characterization of the Type IV Region in Grade 91 Steel Weldments", May 4, 2015, pp9
6. J.G. Nawrocki, J.N. Dupont, C.V. ROBINO, and A.R. MARDER, "The post weld heat-treatment response of simulated coarse-grained heat-affected zones in a new ferritic steel", Metallurgical And Materials Transactions A, 2001, Vol. 32A, pp. 2585-2594.
7. Jonas Ohlsson, "Effects of different heat treatments on hardness of grade 91 steel", Karlstads Univeritet, Faculty of Science and Technology Degree Project for Bachelor of Science in Mechanical Engineering, 2014, pp. 1-32.
8. N. Tammasophon, W. Homhragai, G. Lothongkum " Effect of post weld heat treatment on microstructures and hardness of TIG weldment between P22 and P91 steels with inconel 625 filler metal" Journal of Metals, Materials and Minerals, 2011, vol.21 No.1, pp.93-99.
9. Fujio Abe, Torsten-Ulf Kern and R. Viswanathan, "Creep resistant steels, wood Head Publishing in Material", Cambridge England, 2008, pp. 23, 57 and 477.
10. S. A. David, J. A. Siefert and Z. Feng, "Welding and weldability of candidate ferritic alloys for future advanced ultra-supercritical fossil power plants", Science and Technology of Welding and Joining, 2013, Vol.18, pp. 63.
11. A. Mcgehee and K. Coleman, "Effect of normalization and temper heat treatment on P91 weldment properties", EPRI, interim report, 1004915, 2003, pp. 1-5.
12. Ma. Allam, "Investigation on the influence of welding parameters (Heat input and heat treatments on weldments properties of power boiler steel P91", Cairo University, 2012, pp. 129-145.
13. ASTM E112 "Standard Test Methods for Determining Average Grain Size", pp. 9
14. Genichi Taniguchi, Ken Yamashita, "Effect of post weld heat Treatment temperature on mechanical properties of weld metals for high Cr ferritic heat resistance steel", Kobelco Technology Review, 2013, No. 32, pp. 33-39.

BIOGRAPHIES



Dr. Eisa Salem Mosa, PhD, Eng.
Mining, Metallurgical and Pet. -
Eng. Dept. - Faculty of
Engineering - Al-Azhar
University. Cairo – Egypt